International Journal of Medical Toxicology & Forensic Medicine

2026, Volume 16, E53125

Research Paper

Insular Cortical Thinning and Altered Structural Connectivity in Chronic Cannabis Users: A High-Resolution Morphometry and Diffusion Tractography Study

Fouad Meraji Far[1], Hamid Reza Banafshe[2], Amir Ghaderi[3], Mohammad Ali Atlasi[4]*, Nassim Jalilvand[4]*, Rouhollah Sarollahi[3]*

1. *Alzahra Research Institute, Alzahra University Hospital, Isfahan University of Medical Sciences, Isfahan, Iran*
2. *Physiology Research Center, Institute for Basic Sciences, Kashan University of Medical Sciences, Kashan, Iran*
3. *Clinical Research Development Unit Matini/Kargarnejad Hospitals, Kashan University of Medical Sciences, Kashan, Iran*
4. *Anatomical Sciences Research Center, Institute for Basic Sciences, Kashan University of Medical Sciences, Kashan, Iran*

Citation Meraji Far F, Banafshe HR, Ghaderi A, Atlasi MA, Jalilvand N, Sarollahi R. Insular Cortical Thinning and Altered Structural Connectivity in Chronic Cannabis Users: A High-Resolution Morphometry and Diffusion Tractography Study. International Journal of Medical Toxicology and Forensic Medicine. 2026; 16:E53125.

https://doi.org/10.22037/ijmtfm.v16.53125

Article info:

Received: 07 August, 2026

Accepted: 23 August, 2026

Published: 31 August, 2026

Keywords:

Insular Cortex, Magnetic Resonance Imaging, Cannabis, Addiction, Diffusion Tensor Imaging

ABSTRACT

Background: Available evidence concerning the influence of sustained cannabis use on insular structure remains inconsistent, and comparatively little is known about whether localized cortical alterations coexist with changes in insular white-matter connections. This research investigated the shape of the insula and the structural connectivity centered on the insula in individuals who are chronic cannabis users (CCU).

Methods: A group of twenty-six men, consisting of 13 regular cannabis users and 13 non-users, participated in structural and diffusion MRI scans at 3 Tesla. The YBA-696 parcellation was used to estimate insular thickness and volume at parcel and hemispheric levels, while FreeSurfer provided subcortical volumetric measures. We mapped insular pathways using probabilistic iFOD2 tractography in MRtrix3 and described them by fractional anisotropy, axial diffusivity, mean diffusivity, and radial diffusivity. The data were analyzed using general linear models that incorporated a comprehensive set of relevant covariates, with the Benjamini–Hochberg procedure subsequently applied to control the family-wise error rate by controlling the false discovery rate.

Results: Compared with controls, cannabis users exhibited thinner cortices in both insulae, with eight individual parcels remaining significant after false-discovery-rate correction. Insular volume was similar across groups. Additionally, cannabis users showed reduced total gray-matter volume and smaller brainstem, right thalamus, left cerebellar cortex, left amygdala, and right orbitofrontal gyrus volumes. Connectivity analyses demonstrated lower mean diffusivity in the left insula-amygdala pathway, additional parcel-specific abnormalities within this system, and lower fractional anisotropy in connections linking the right insula to the hippocampus and precentral gyrus, and the left insula to occipital regions.

Conclusion: Rather than inducing generalized atrophy of the insula, long-term cannabis exposure was associated with focal cortical thinning in this region and selective microstructural changes confined primarily to limbic and cortical pathways. These findings implicate networks involved in salience, affective processing, and sensorimotor integration. Because the study was cross-sectional, larger longitudinal investigations are needed to establish the direction and clinical relevance of these associations.

*** Corresponding Authors:**

Mohammad Ali Atlasi, PhD, Anatomical Sciences Research Center, Institute for Basic Sciences, Kashan University of Medical Sciences, Kashan, Iran. E-mail: *atlasima@gmail.com.* ***AND Nassim Jalilvand, PhD; Anatomical Sciences Research Center, Institute for Basic Sciences, Kashan University of Medical Sciences, Kashan, Iran. E-mail:*** *n.jalilvand1980@gmail.com.* ***AND Rouhollah Sarollahi, PhD; Clinical Research Development Unit Matini /Kargarnejad Hospitals, Kashan University of Medical Sciences, Kashan, Iran. E-mail:*** *sarollahy@gmail.com*

Introduction

As the most commonly consumed illicit drug worldwide, cannabis has drawn growing scholarly attention, chiefly owing to mounting apprehension regarding the enduring neurobiological ramifications of sustained use [1]. Repeated cannabis use can progress to cannabis use disorder, characterized by persistent drug-seeking and impaired control despite adverse consequences [2]. The salience network is central to these processes because it integrates internal and external signals that guide attention, motivation, and behavioral responses [3]. The insular cortex, a major hub of this network, contributes to interoception, craving, reward processing, and the integration of emotionally salient information [4].

Structural MRI studies examining cannabis-related neuroanatomical changes have produced inconsistent findings, particularly regarding insular cortical thickness and gray-matter volume. Differences in participant characteristics, comorbid substance use, imaging methodology, and analytic resolution may partly explain these discrepancies. In addition, although functional abnormalities of the insula are well documented in addiction, relatively little evidence has examined the structural integrity of white matter pathways connecting the insula to cortical and subcortical regions involved in reward, affective processing, memory, and behavioral control [5, 6].

The current research examined both the morphology of the insula and the structural connectivity centered around the insula in individuals who use cannabis chronically, compared to matched control subjects. We used high-resolution cortical parcellation to assess insular thickness and volume, while diffusion MRI tractography quantified microstructural properties of insula–cortical and insula–subcortical pathways. We proposed that long-term cannabis consumption would correlate with specific morphometric changes in the insula and targeted disruption of the structural connections that link the insula to limbic and cortical areas related to salience and valuation.

Materials and Methods

Investigative strategy

We conducted a case-control MRI study comparing 13 men with CCU and 13 male non-user controls. Sample size was estimated from previously reported mean and standard deviation values for insular cortical thickness, yielding a minimum of 13 participants per group [7]. Recruitment proceeded through two routes. The first recruitment pool originated from an earlier survey of 2,183 individuals, 329 of whom indicated that they would consider participating in brain imaging. Screening identified 28 potential CCUs. Five cannabis users and 10 controls recruited through this pathway completed the imaging protocol. Community recruitment subsequently provided another eight cannabis users and three controls, resulting in a final sample of 26 participants.

Participants were classified as CCU when they reported at least 10 cannabis-use occasions per month over a period of two years or longer. Participants reporting use of substances other than cannabis or cigarettes more than once per month were excluded. Other exclusion criteria were hypertension, previous brain surgery, psychiatric disorders, neuropsychiatric medication use, alcohol use, epilepsy, autism, claustrophobia, metal implants, attempted suicide, self-harm, and reported histories of sexual assault or childhood abuse. Eligibility was assessed by self-report.

MRI Acquisition

Magnetic resonance imaging was performed on all participants using a 3-T Siemens Prisma system, equipped with a 20-channel phased-array head coil. For anatomical reference, a three-dimensional sagittal MPRAGE sequence was employed, with imaging parameters set as follows: TR = 2,300 ms, TE = 2.98 ms, TI = 900 ms, flip angle = 9°, slice count = 176, and isotropic spatial resolution = 1 mm^3. Diffusion-sensitized data were subsequently acquired using a single-shot spin-echo EPI sequence, with TR = 7,600 ms and TE = 89 ms, and a voxel size of 1.8 mm^3 isotropic. The diffusion protocol consisted of 60 non-collinear gradient directions at b = 1,500 s/mm^2, along with non-diffusion-weighted images. Images with opposing anterior-to-posterior and posterior-to-anterior phase encoding were obtained to support susceptibility-distortion correction. All anatomical and diffusion images underwent visual assessment for gross motion, acquisition failure, and other artifacts before processing.

Morphometric Analysis

Cortical reconstruction and subcortical segmentation were performed on the T1-weighted data with FreeSurfer 7.8.0 and its recon-all workflow [8]. The resulting surfaces and anatomical labels were visually reviewed before quantitative measures were exported. FreeSurfer provided the subcortical volumes

and estimated total intracranial volume used in subsequent analyses. Insular measurements were obtained from the 696-region Yale Brain Atlas parcellation [9]. Insular parcels were analyzed individually and combined to derive hemisphere-specific whole-insula measurements. Non-insular atlas parcels were assigned to prespecified cortical macroregions using their anatomical locations and published descriptions of insular connectivity [10, 11].

Diffusion Processing and Tractography

Diffusion processing was undertaken with FSL 6.0.7.19 and MRtrix3 3.0.8 [12, 13]. Susceptibility-related displacement was estimated from the reverse-phase data with TOPUP. Eddy-current distortion and participant motion were then corrected with eddy, followed by ANTs-based bias-field correction. Tensor estimation generated maps of fractional anisotropy, axial diffusivity, mean diffusivity, and radial diffusivity.

The predefined anatomical parcellations were transformed into the diffusion space native to each individual participant. To maintain the discrete, non-continuous identity of the insular and cortical territories defined by the YBA atlas, a nearest-neighbor interpolation strategy was applied during the resampling process. Bilateral volumetric masks representing the thalamus, caudate nucleus, putamen, globus pallidus, hippocampus, amygdala, and nucleus accumbens were derived from automated segmentations performed using FreeSurfer. Estimation of fiber-orientation distributions was performed using single-shell constrained spherical deconvolution. Subsequently, whole-brain probabilistic fiber tracking was executed employing the iFOD2 algorithm, all within a tractography framework constrained by anatomical priors. The initiation of streamline propagation was positioned precisely at the cortical gray–white matter junction. For each reconstructed pathway linking the insula to its designated target structures, diffusivity metrics, including FA, MD, AD, and RD, were extracted along the surviving streamlines and subsequently averaged, yielding summary diffusion measures for each individual connection.

Statistical Analysis

All analyses were performed using R version 4.5.2. Between-group contrasts were examined using general linear models that included age, BMI, and estimated total intracranial volume as covariates, as appropriate for the outcome. Streamline-count measures were log-transformed before modeling to address distributional skewness. Multiplicity was managed separately within each prespecified family of tests using the Benjamini–Hochberg false discovery rate method. Adjusted q values below 0.05 were interpreted as statistically significant. Effect sizes and their corresponding 95% confidence intervals were provided for findings that met this criterion.

Results

Participant characteristics

The final cohort consisted of 26 men, equally divided between the cannabis and control groups. Mean age was 24.5 ± 4.7 years among cannabis users and 25.7 ± 4.7 years among controls; no statistically significant age difference was detected (p=0.510). Mean BMI was 23.6 ± 3.5 and 22.6 ± 2.3 kg/m², respectively (p=0.402).

Table 1. Participants characteristics (N=13, all male).

Group	Age (years) (mean ± SD)	BMI (kg/m²) (mean ± SD)	Welch's p
Cannabis	24.5 ± 4.7	23.6 ± 3.5	0.510
Control	25.7 ± 4.7	22.6 ± 2.3	0.402

International Journal of
Medical Toxicology & Forensic Medicine

Note. BMI denotes body mass index and was calculated as weight in kilograms divided by height in meters squared (kg/m²). Between-group comparisons were performed using Welch's two-sample *t-test*.

Participant characteristics are summarized in Table 1.

Global, cortical, and subcortical morphometry

The groups did not exhibit any statistically significant differences in estimated total intracranial volume. Cannabis users had lower total gray-matter volume than controls (660,906.8±55,636.1 vs 694,086.6±58,823.0 mm³; p=0.036, q_FDR=0.036). No significant differences were detected in total cerebral white-matter volume or composite brain-segmentation measures. Regional volume reductions in cannabis users involved the brainstem (19,891.2±2,006.3 vs 21,996.1±1,706.3 mm³; q_FDR=0.008), left amygdala (1,716.3±179.7 vs 1,861.4±160.4 mm³; q_FDR=0.033), right thalamus (7,843.2±1,213.3 vs 8,547.6±571.4 mm³; q_FDR=0.037), left cerebellar cortex (55,058.0±7,010.5 vs 58,312.6±6,650.1 mm³; q_FDR=0.049), and right orbitofrontal gyrus (10,006.8±616.1 vs 11,388.6±1,516.0 mm³; q_FDR=0.035). No other regional volume or macro-regional cortical-thickness differences survived FDR correction (Table 2).

Insular morphometry

Whole-insula volumes were not significantly different (Table 3). In direct opposition, mean cortical

Table 2. Global and regional brain-volume differences that remained significant after FDR correction.

Anatomical domain	Measure	Cannabis mean ± SD	Control mean ± SD	p	q_FDR
Global	Total gray-matter volume	660906.8 ± 55636.1	694086.6 ± 58823.0	0.036	0.036
Cortical	Right orbitofrontal gyrus	10006.8 ± 616.1	11388.6 ± 1516.0	0.001	0.035
Subcortical	Left amygdala	1716.3 ± 179.7	1861.4 ± 160.4	0.033	0.033
Subcortical	Right thalamus	7843.2 ± 1213.3	8547.6 ± 571.4	0.037	0.037
Infratentorial	Brainstem	19891.2 ± 2006.3	21996.1 ± 1706.3	0.008	0.008
Infratentorial	Left cerebellar cortex	55058.0 ± 7010.5	58312.6 ± 6650.1	0.049	0.049

Note. Values are group means ± SD in mm³. q_FDR denotes Benjamini-Hochberg-adjusted p values; q_FDR < 0.05 was considered significant.

Table 3. Hemispheric profile of whole-insula volume and cortical thickness.

/	Measure	Unit	Cannabis mean ± SD	Control mean ± SD	p	q_FDR
Left	Volume	mm³	4816.8 ± 550.3	4751.1 ± 447.6	0.741	0.741
Left	Cortical thickness	mm	3.062 ± 0.280	3.409 ± 0.196	0.001	0.005
Right	Volume	mm³	4673.8 ± 565.9	4982.8 ± 1154.3	0.398	0.597
Right	Cortical thickness	mm	3.034 ± 0.295	3.347 ± 0.207	0.005	0.010
Bilateral	Total volume	mm³	9490.6 ± 990.4	9733.8 ± 1379.9	0.611	0.733
Bilateral	Mean thickness	mm	3.048 ± 0.279	3.378 ± 0.173	0.002	0.005

Note. Values are group means ± SD. The bilateral summary is reported as total volume and mean thickness. q_FDR values were obtained using the Benjamini-Hochberg adjustment.

thickness was lower in cannabis users in the left insula (3.062±0.280 vs 3.409±0.196 mm; p=0.001, q_FDR=0.005), right insula (3.034±0.295 vs 3.347±0.207 mm; p=0.005, q_FDR=0.010), and bilateral mean (3.048±0.279 vs 3.378±0.173 mm; p=0.002, q_FDR=0.005). Parcel-wise analysis identified eight parcels with significantly lower thickness: L_I1_A, L_I4_A, L_I4_C, L_I5_C, R_I3_A, R_I3_C, R_I4_B, and R_I5_B (q_FDR=0.002–0.044). Thickness reductions were approximately 0.30–0.70 mm. The spatial distribution of these significant parcels is illustrated in Figure 1. No parcel-level insular volume difference survived correction (Table 4).

Insula–subcortical structural connectivity

At the whole-region level, the only FDR-significant result was observed for mean diffusivity in the left insula–amygdala connection. Mean diffusivity was 0.972±0.050×10⁻³ mm²/s in cannabis users and 1.031±0.051×10⁻³ mm²/s in controls (p=0.014,

Table 4. YBA insular parcels with FDR-significant cortical thinning, ordered by hemisphere and mean difference.

Hemisphere	YBA parcel	Cannabis mean ± SD, mm	Control mean ± SD, mm	Mean difference* mm	p	q_FDR
Left	L_I4_C	3.09 ± 0.44	3.79 ± 0.31	-0.70	<0.001	0.002
Left	L_I5_C	3.01 ± 0.41	3.63 ± 0.40	-0.62	<0.001	0.003
Left	L_I1_A	2.88 ± 0.32	3.23 ± 0.29	-0.35	0.005	0.030
Left	L_I4_A	2.47 ± 0.17	2.77 ± 0.32	-0.30	0.002	0.014
Right	R_I5_B	2.66 ± 0.50	3.32 ± 0.49	-0.66	0.005	0.030
Right	R_I3_C	3.55 ± 0.64	4.06 ± 0.48	-0.51	0.009	0.043
Right	R_I4_B	2.78 ± 0.51	3.23 ± 0.39	-0.45	0.010	0.044
Right	R_I3_A	2.68 ± 0.26	2.98 ± 0.20	-0.30	0.002	0.014

Note. *Mean difference was calculated as the cannabis-group mean minus the control-group mean; negative values indicate lower thickness in cannabis users. Parcel labels correspond to the YBA parcellation in Figure 1. q_FDR values were adjusted using the Benjamini-Hochberg procedure.

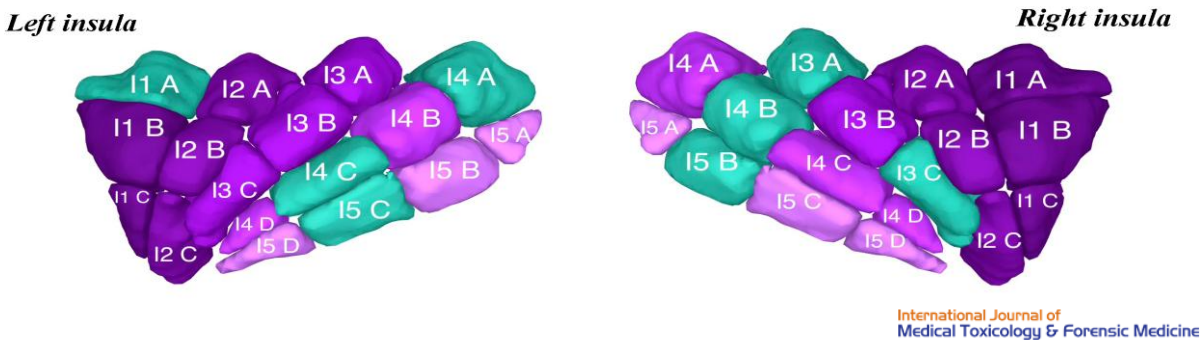

Figure 1. Three-dimensional YBA parcellation of the left and right insulae. Atlas-defined subdivisions are identified by their parcel labels, and regions demonstrating significant between-group differences in cortical thickness after FDR correction are highlighted in green.

q_FDR=0.041). FA, AD, and RD for this whole-insula connection did not meet the adjusted significance threshold, and no other whole-region insula–subcortical comparison was significant after correction. The finer parcel-level analysis identified a cluster of findings involving the left amygdala. Compared with controls, cannabis users had higher FA in the L_I2_B–amygdala connection (0.291±0.059 versus 0.221±0.034; q_FDR=0.019). Lower diffusivity values were found for: MD in the L_I2_B–, L_I4_A– and L_I5_A–amygdala connections, AD in the L_I3_C–, L_I4_A– and L_I5_A–amygdala connections, and RD in the L_I2_B– and L_I5_A–amygdala connections. The adjusted *q* values for these left-sided parcel-level findings ranged from 0.026 to 0.039. In the right hemisphere, FA was lower for the R_I5_C–hippocampus connection in the cannabis group (0.234±0.042 versus 0.394±0.073; *p*=0.005, q_FDR=0.050). Complete estimates are provided in Table 5, and the reconstructed insular connectome is illustrated in Figure 2.

Insula–cortical structural connectivity

In the left hemisphere, ROI-level FA was lower in cannabis users for insula connections with the lateral occipital fusiform gyrus (0.434 ± 0.026 vs 0.469 ± 0.021; q_FDR = 0.011), medial occipital fusiform gyrus (0.444 ± 0.049 vs 0.487 ± 0.017; q_FDR = 0.043), and posterior lingual gyrus (0.468 ± 0.041 vs 0.504 ± 0.023; q_FDR = 0.043). Edge-wise analysis identified higher RD in the L_I4_A–medial fusiform connection (q_FDR = 0.021). In the right hemisphere, no ROI-level differences survived correction; however, FA was lower in the R_I5_A–

Table 5. Insula-subcortical connectivity: ROI summary and FDR-significant parcel-level findings.

Analysis level	Insula-subcortical connection	Metric	Cannabis mean ± SD	Control mean ± SD	p	q_FDR
ROI level	Left whole insula-amygdala	FA	0.228 ± 0.030	0.215 ± 0.022	0.413	0.413
ROI level	Left whole insula-amygdala	MD	0.972 ± 0.050	1.031 ± 0.051	0.014	0.041
ROI level	Left whole insula-amygdala	AD	1.188 ± 0.044	1.247 ± 0.065	0.019	0.057
ROI level	Left whole insula-amygdala	RD	0.864 ± 0.056	0.924 ± 0.048	0.018	0.053
Parcel level	L_I2_B-amygdala	FA	0.291 ± 0.059	0.221 ± 0.034	0.001	0.019
Parcel level	L_I2_B-amygdala	MD	0.887 ± 0.033	1.049 ± 0.156	0.008	0.039
Parcel level	L_I2_B-amygdala	RD	0.753 ± 0.054	0.937 ± 0.153	0.003	0.035
Parcel level	L_I3_C-amygdala	AD	1.160 ± 0.079	1.352 ± 0.014	0.006	0.026
Parcel level	L_I4_A-amygdala	MD	0.988 ± 0.098	1.100 ± 0.077	0.006	0.039
Parcel level	L_I4_A-amygdala	AD	1.186 ± 0.087	1.303 ± 0.082	0.002	0.026
Parcel level	L_I5_A-amygdala	MD	0.911 ± 0.096	1.113 ± 0.107	0.004	0.039
Parcel level	L_I5_A-amygdala	AD	1.119 ± 0.103	1.336 ± 0.121	0.004	0.026
Parcel level	L_I5_A-amygdala	RD	0.807 ± 0.097	1.002 ± 0.107	0.005	0.035
Parcel level	R_I5_C-hippocampus	FA	0.234 ± 0.042	0.394 ± 0.073	0.005	0.050

International Journal of
Medical Toxicology & Forensic Medicine

Note. FA is dimensionless; MD, AD, and RD are expressed in ×10⁻³ mm²/s. Whole insula indicates a hemisphere-wide seed. ROI-level rows provide all four-diffusion metrics for the left insula-amygdala connection, whereas parcel-level rows are limited to findings retained after FDR adjustment. q_FDR values were adjusted using the Benjamini-Hochberg procedure.

Table 6. FDR-significant insula-cortical connectivity differences organized by analysis level.

Analysis level	Insula-cortical connection	Metric	Cannabis mean ± SD	Control mean ± SD	p	q_FDR
ROI level	Left whole insula-lateral fusiform	FA	0.434 ± 0.026	0.469 ± 0.021	0.001	0.011
ROI level	Left whole insula-medial fusiform	FA	0.444 ± 0.049	0.487 ± 0.017	0.010	0.043
ROI level	Left whole insula-posterior lingual	FA	0.468 ± 0.041	0.504 ± 0.023	0.013	0.043
Parcel level	L_I4_A-medial fusiform	RD	0.666 ± 0.010	0.527 ± 0.001	<0.001	0.021
Parcel level	R_I5_A-precentral gyrus	FA	0.281 ± 0.044	0.359 ± 0.044	<0.001	0.050

Note. FA is dimensionless, and RD is expressed in $\times 10^{-3}$ mm²/s. Whole insula indicates a hemisphere-wide seed. All displayed rows met the reported FDR criterion, with q_FDR values adjusted using the Benjamini-Hochberg procedure. Parcel labels correspond to Figure 1.

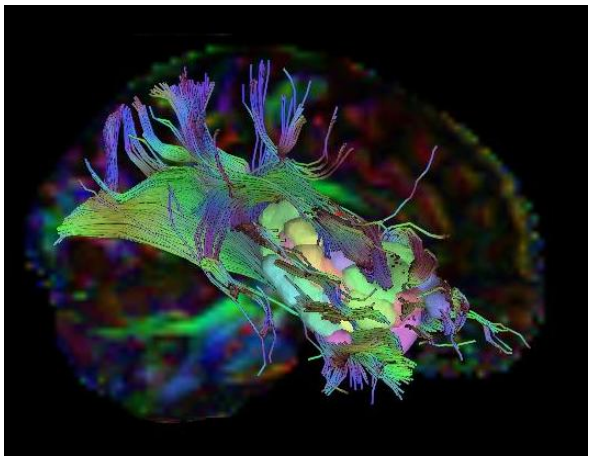

Figure 2. Sagittal visualization of the right insular structural connectome derived from diffusion MRI tractography. Streamlines generated using a high-angular-resolution diffusion imaging (HARDI) approach depict pathways linking the right insula to cortical and subcortical regions and are displayed over the corresponding anatomical image. Fiber colors encode the principal diffusion orientations, illustrating the organization of white-matter pathways associated with the insula.

precentral gyrus edge (0.281 ± 0.044 vs 0.359 ± 0.044; q_FDR = 0.050). No other insula–cortical effects survived FDR correction (Table 6).

Discussion

The principal finding of this study was bilateral insular cortical thinning in CCU, detectable both at the whole-insula level and within several high-resolution YBA parcels, despite preserved insular volume. This pattern suggests that cortical thickness may be more sensitive than regional volume to subtle structural differences associated with chronic cannabis exposure. Because cortical volume reflects both thickness and surface area, focal thinning can occur without measurable volumetric loss, particularly in small samples. Previous structural MRI studies of cannabis use have reported heterogeneous findings, likely reflecting differences in age, dependence severity, comorbid substance use, imaging methods, and analytic resolution [14-16]. Our parcel-based approach may therefore have detected localized insular effects that are diluted in broader whole-brain or atlas-level analyses.

In individuals who consume cannabis, neuroimaging studies indicate diminished total gray matter volume, as well as reductions in specific regions, including the right orbitofrontal gyrus, right thalamus, left amygdala, brainstem, and left cerebellar cortex. These regions contribute to reward valuation, affective salience, arousal, sensory integration, and cognitive control and are frequently implicated in addiction-related neurocircuitry. The orbitofrontal cortex and amygdala are particularly relevant because both are involved in incentive valuation and emotional learning and are enriched in cannabinoid receptors. However, large multisite studies have not consistently identified the same regional abnormalities [14, 16, 17]. Consequently, these results should be viewed as evidence of specific structural variations in different regions, rather than as a consistent neuroanatomical characteristic of cannabis consumption.

The findings from the tractography analysis indicate that CCU is linked to changes in the microstructural organization of insula-centered neural networks. At the level of regions of interest (ROI), the left insula–amygdala pathway exhibited a reduced mean diffusivity. Furthermore, parcel-level analyses revealed additional decreases in both axial and radial diffusivity, alongside an increase in fractional anisotropy (FA) within specific insula–amygdala connections. A right insula–hippocampus connection also showed lower FA. These pathways support the integration of interoceptive, emotional, contextual, and reward-related information, processes relevant to craving and habitual drug use. Nevertheless, diffusion measures such as FA, MD, AD, and RD are biologically nonspecific and can be influenced by crossing fibers, tract geometry, and streamline selection. Thus, the present findings are best interpreted as altered white-matter microstructure rather than direct evidence of changes in myelination or axonal density.

We also observed reduced FA in left insula connections with occipital fusiform and posterior lingual regions and in a right insula–precentral connection. These selective cortical effects may reflect altered coupling between salience processing and visual or sensorimotor systems, which may be relevant to cue-driven attention and behavioral responses. Their modest magnitude and the reduced sample size for some tract estimates, however, require cautious interpretation and independent replication.

The pattern of focal cortical thinning and selective tract abnormalities is broadly compatible with an endocannabinoid-linked vulnerability model. Prior studies have reported associations between cannabis-related cortical changes and regional CB1 receptor availability or endocannabinoid-related molecular markers [18]. Because the insula, orbitofrontal cortex, and amygdala participate in salience, interoception, and valuation, structural alterations within this network may contribute to dysregulated cue processing and impaired behavioral control.

The sample was small, male-only, and cross-sectional, limiting generalizability and statistical power. Cannabis potency, age at onset, abstinence duration, and nicotine exposure were not modeled in sufficient detail to assess dose-response effects. In addition, some tractography estimates were unavailable for all participants. Larger longitudinal studies with detailed exposure phenotyping and advanced diffusion methods are needed to determine whether these insular and network-level abnormalities represent consequences of chronic cannabis exposure, pre-existing vulnerability, or adaptive remodeling. Despite these limitations, the convergence of morphometric and tractography findings supports further investigation of the insula as a potentially sensitive structural marker of chronic cannabis exposure.

Conclusion

CCU was associated with selective structural brain alterations, most prominently bilateral insular cortical thinning without significant insular volume loss. Additional reductions were observed in total gray matter and several addiction-relevant regions, including the amygdala, thalamus, cerebellar cortex, brainstem, and orbitofrontal cortex. Diffusion tractography further revealed altered microstructural organization in insula-centered pathways, particularly in connections to the amygdala, hippocampus, occipital cortex, and precentral gyrus. Together, these findings suggest that chronic cannabis exposure may preferentially affect neural circuits involved in salience processing, interoception, affective valuation, and sensorimotor integration. The coexistence of focal cortical thinning and selective connectivity abnormalities supports an endocannabinoid-linked vulnerability model. However, larger longitudinal studies are required to determine causality and clarify the clinical significance of these structural changes.

Ethical Approval

Prior to MRI scanning and study inclusion, written informed consent was secured from every participant. The study procedures were duly authorized by the Ethics Committee of Kashan University of Medical Sciences (IR.KAUMS.MEDNT.REC.1401.015).

Acknowledgment

The Clinical Research Development Unit of Matini/Kargarnejad Hospitals and Kashan University of Medical Sciences provided institutional support for the project. MRI acquisition was facilitated by the National Brain Mapping Laboratory. The authors also acknowledge assistance from the Clinical Research Development Unit of Kashan Shahid Beheshti Hospital and the Narcotics Control Headquarters of Isfahan Province. We thank the study participants for their time and cooperation.

Funding

Kashan University of Medical Sciences provided financial support for the present study (No: 400158). It is important to note that the funding institution did not contribute to any aspect of the study, including subject recruitment, image collection, data analysis, interpretation of results, manuscript writing, or the submission process.

Conflicts of Interest

There are no competing interests to declare.

References

[1] Sarollahi R, Ghaderi A, Banafshe HR, Atlasi MA. Lifetime, last month and excessive prevalence of addictive substances consumption among the general population and university students in the city of Tehran. Int J High Risk Behav Addict. 2025;14(3). [DOI: 10.5812/ijhrba-159843]

[2] Albaugh MD, Ottino-Gonzalez J, Sidwell A, Lepage C, Juliano A, Owens MM, et al. Association of cannabis use during adolescence with neurodevelopment. JAMA Psychiatry. 2021;78(9):1031-40. [DOI: 10.1001/jamapsychiatry.2021.1258]

[3] Chen T, Cai W, Ryali S, Supekar K, Menon V. Distinct global brain dynamics and spatiotemporal organization of the salience network. PLoS Biol. 2016;14(6). [DOI: 10.1371/journal.pbio.1002469]

[4] Li C, Pang X, Shi K, Long Q, Liu J, Zheng J. The insula is a hub for functional brain network in patients with anti-N-methyl-D-aspartate receptor encephalitis. Front Neurosci. 2021;15:642390. [DOI: 10.3389/fnins.2021.642390]

[5] Koenis MMG, Durnez J, Rodrigue AL, Mathias SR, Alexander-Bloch AF, Barrett JA, et al. Associations of cannabis use disorder with cognition, brain structure, and brain function in African Americans. Hum Brain Mapp. 2021;42(6):1727-41. [DOI: 10.1002/hbm.25324]

[6] Mackey S, Allgaier N, Chaarani B, Spechler P, Orr C, Bunn J, et al. Mega-analysis of gray matter volume in substance dependence: General and substance-specific regional effects. Am J Psychiatry. 2019;176(2):119-28. [DOI: 10.1176/appi.ajp.2018.17040415]

[7] Livny A, Cohen K, Tik N, Tsarfaty G, Rosca P, Weinstein A. The effects of synthetic cannabinoids (SCs) on brain structure and function. Eur Neuropsychopharmacol. 2018;28(9):1047-57. [DOI: 10.1016/j.euroneuro.2018.07.095]

[8] Fischl B. FreeSurfer. Neuroimage. 2012;62(2):774-81. [DOI: 10.1016/j.neuroimage.2012.01.021]

[9] McGrath H, Zaveri HP, Collins E, Jafar T, Chishti O, Obaid S, et al. High-resolution cortical parcellation based on conserved brain landmarks for localization of multimodal data to the nearest centimeter. Sci Rep. 2022;12(1):18778. [DOI: 10.1038/s41598-022-21543-3]

[10] Ghaziri J, Tucholka A, Girard G, Boucher O, Houde JC, Descoteaux M, et al. Subcortical structural connectivity of insular subregions. Sci Rep. 2018;8(1):8596. [DOI: 10.1038/s41598-018-26995-0]

[11] Makris N, Rushmore R, Kaiser J, Albaugh M, Kubicki M, Rathi Y, et al. A proposed human structural brain connectivity matrix in the Center for Morphometric Analysis Harvard-Oxford Atlas Framework: A historical perspective and future direction for enhancing the precision of human structural connectivity with a novel neuroanatomical typology. Dev Neurosci. 2023;45(4):161-80. [DOI: 10.1159/000530358]

[12] Jenkinson M, Beckmann CF, Behrens TEJ, Woolrich MW, Smith SM. FSL. Neuroimage. 2012;62(2):782-90. [DOI: 10.1016/j.neuroimage.2011.09.015]

[13] Tournier JD, Smith RE, Raffelt D, Tabbara R, Dhollander T, Pietsch M, et al. MRtrix3: A fast, flexible and open software framework for medical image processing and visualisation. Neuroimage. 2019;202:116137. [DOI: 10.1016/j.neuroimage.2019.116137]

[14] Chye Y, Mackey S, Gutman BA, Ching CRK, Batalla A, Blaine S, et al. Subcortical surface morphometry in substance dependence: An ENIGMA Addiction Working Group study. Addict Biol. 2020;25(6). [DOI: 10.1111/adb.12830]

[15] Lorenzetti V, Chye Y, Silva P, Solowij N, Roberts CA. Does regular cannabis use affect neuroanatomy? An updated systematic review and meta-analysis of structural neuroimaging studies. Eur Arch Psychiatry Clin Neurosci. 2019;269(1):59-71. [DOI: 10.1007/s00406-019-00979-1]

[16] Lorenzetti V, Gaillard A, McTavish E, Grace S, Rossetti MG, Batalla A, et al. Cannabis dependence is associated with reduced hippocampal subregion volumes independently of sex: Findings from an ENIGMA Addiction Working Group multi-country study. Cannabis Cannabinoid Res. 2024;9(6). [DOI: 10.1089/can.2023.0204]

[17] Cao Z, Ottino-Gonzalez J, Cupertino RB, Schwab N, Hoke C, Catherine O, et al. Mapping cortical and subcortical asymmetries in substance dependence: Findings from the ENIGMA Addiction Working Group. Addict Biol. 2021;26(5). [DOI: 10.1111/adb.13010]

[18] Manza P, Yuan K, Shokri-Kojori E, Tomasi D, Volkow ND. Brain structural changes in cannabis dependence: Association with MAGL. Mol Psychiatry. 2020;25(12):3256-66. [DOI: 10.1038/s41380-019-0577-z]